Sensors and Materials, Vol. 28, No. 11 (2016) 1179–1189
MYU Tokyo

S & M 1279

Acetone-Sensing Properties of WO_3-Based Gas Sensors Operated in Dynamic Temperature Modulation Mode —Effects of Loading of Noble Metal and/or NiO onto WO_3—

Takeo Hyodo,* Takuya Kaino, Taro Ueda, Kuniyuki Izawa,[1] and Yasuhiro Shimizu

Graduate School of Engineering, Nagasaki University, 1-14 Bunkyo-machi, Nagasaki 852-8521, Japan
[1]Figaro Engineering Inc., 1-5-11 Senbanishi, Minoo, Osaka 562-8505, Japan

(Received April 27, 2016; accepted July 25, 2016)

Keywords: acetone, dynamic temperature modulation, semiconductor gas sensor, WO_3, hydrogen

Micro gas sensors fabricated with WO_3 loaded with and without a noble metal and/or NiO as a sensing material were operated in dynamic temperature modulation mode with sinusoidal modulation of Pt-heater voltage [low voltage: 0 V for RT, maximum voltage: 0.6 V (for 150 °C)–1.6 V (for 400 °C), period: 6 s], and their acetone-sensing properties were investigated in dry and wet air. The WO_3 sensor showed negligible dynamic responses to acetone and H_2, but the loading of a noble metal onto the WO_3 markedly improved the dynamic responses, particularly to acetone in dry air. Among all the 0.5 wt% noble-metal-loaded WO_3 (0.5*N*/WO_3, *N*: noble metal) sensors tested, the 0.5Pt/WO_3 sensor showed the largest dynamic response to acetone in dry air, while the dynamic response to acetone was largely decreased by the addition of moisture into the gaseous atmosphere. The loading of NiO onto WO_3 and 0.5Pt/WO_3 improved the dynamic response to acetone of the WO_3 and 0.5Pt/WO_3 sensors, and the 1.0 wt% NiO-loaded 0.5Pt/WO_3 sensor showed the largest dynamic acetone response and dynamic acetone selectivity against H_2. These acetone-sensing properties of the sensors operated in dynamic temperature modulation mode were superior to those of the ones operated in static constant temperature mode, possibly because of acetone and/or its partial oxidation products adsorbed on the oxide surface at low temperatures and their abrupt catalytic combustion with oxygen adsorbates at high temperatures.

1. Introduction

It is well known that human exhaled breath contains various types of gaseous species with high humidity, and that qualitative and quantitative analyses of the gases enable us to estimate health conditions and to diagnose various diseases. For example, the concentration of methane and hydrogen in exhaled breath increases with the growth of anaerobic bacteria in the large intestine,[1–3] and thus their monitoring is useful for diagnosing the digestive and absorptive functions of carbohydrates. As volatile sulfur compounds such as methyl mercaptan and hydrogen sulfide are produced in the mouth by oral bacteria,[4,5] the quantitative analysis of these compounds is helpful in diagnosing halitosis originating from periodontal disease in dental clinics. Relatively large amounts of ammonia,[6] nitrogen monoxide,[7] pentane,[8] toluene,[9,10] and 1-nonanal[11] are also known to be detected in the exhaled breath of patients with kidney disorder, asthma, heart disease, and lung

*Corresponding author: e-mail: hyodo@nagasaki-u.ac.jp

ISSN 0914-4935

cancer, respectively, and thus the development of breakthrough gas-sensing devices that can detect these gases sensitively and selectively has been expected for the early-stage detection of these diseases.

Acetone is produced in exhaled breath by the fat-burning process during weight-loss diet and exercise,[12] and it is also one of the representative biomarkers contained in the exhaled breath of diabetic patients.[13] Therefore, many researchers have attempted to develop highly sensitive and selective semiconductor-type acetone sensors by utilizing various types of metal oxides as acetone-sensing materials.[10,14–23] For example, Righettoni *et al.* have reported that the loading of 10 mol% Si-based components onto WO_3 largely improved the acetone-sensing properties of the WO_3 sensor.[15,16] Wang *et al.* have demonstrated that a 10 mol% Cr_2O_3-loaded WO_3 sensor showed a relatively large response to acetone, in comparison with responses to other gases such as ethanol, isoprene, and nitrogen monoxide.[17] Xie *et al.* have clarified that the compositional and structural control of ZnO–CuO composite sensors effectively improved the acetone selectivity against toluene, ethanol, and methanol.[23] On the other hand, the operation of gas sensors in dynamic temperature modulation mode is quite effective in enhancing gas-sensing properties,[24–34] particularly for volatile organic compounds (VOCs). Our group has actually demonstrated that catalytic combustion-type gas sensors that were operated in a mode of pulsed temperature heating (typical pulsed-heating period: 400 ms for 10 s), so-called adsorption/combustion-type gas sensors, showed large dynamic responses to various types of VOCs.[35–40] In this work, we have attempted to improve the acetone-sensing properties of WO_3-based sensors, particularly in wet air, by the loading of noble metal and/or NiO onto the surface of WO_3, as well as by operation in dynamic temperature modulation mode.

2. Experimental Procedure

2.1 Preparation of WO_3 powders loaded with and without noble metal and/or NiO

HNO_3 aq. (0.10 mol dm^{-3}, 10 cm^3) was added dropwise into a Na_2WO_4 aqueous solution (0.15 mol/L, 100 cm^3), and then the yellow resultant precipitate was calcined at 500 °C for 2 h in air. It was confirmed that the crystal structure of the prepared powder was monoclinic WO_3 (JCPDS No. 43-1035) by X-ray diffraction analysis (XRD; Rigaku Corp., RINT2200) using Cu Kα radiation (40 kV, 36 mA). In addition, the specific surface area, which was measured by the general Brunauer–Emmett–Teller (BET) method using a N_2 adsorption isotherm (Micromeritics Inst. Corp., TriStar 3000), was ca. 11.6 m^2 g^{-1}. The WO_3 powder was impregnated with an appropriate amount of $Ni(NO_3)_2$ aqueous solution (0.07 mol/L), followed by calcination at 500 °C for 2 h in air. The obtained NiO-loaded WO_3 powders were denoted as *m*NiO/WO_3 [*m*: amount of NiO loading, 1.0, 5.0, and 10 (wt%)]. In addition, an appropriate amount of WO_3 or *m*NiO/WO_3 powder was added into $RuCl_3$ (8.5×10^{-3} mol dm^{-3}), $PtCl_4$ (1.5×10^{-2} mol dm^{-3}), $Pd(NO_3)_2$ (2.1×10^{-2} mol dm^{-3}), or $HAuCl_4$ aq. (1.5×10^{-2} mol dm^{-3}) aqueous solution. After they were ultrasonicated at RT for 1 h, they were evaporated to dryness at 100 °C for 2 h in air. The resultant solids were heat-treated at 200 °C for 2 h in H_2, followed by calcination at 500 °C for 2 h in air. The obtained WO_3 and *m*NiO/WO_3 powders loaded with noble metal (*N*) were denoted as *nN*/WO_3 and *nN*/*m*NiO/WO_3 [*n*: amount of noble metal (*N*: Au, Pd, Pt, or Ru), 0.1, 0.5, and 1.0 (wt%)].

2.2 Fabrication of micro gas sensors and measurement of gas-sensing properties

Figure 1 shows a top view of a typical micro gas sensor fabricated by utilizing WO_3 as a gas-sensing material and a cross-sectional schematic drawing of micro gas sensors fabricated in this study. The paste containing the obtained powder and an appropriate amount of terpineol were applied onto interdigitated Pt electrodes attached on a microsensor chip fabricated by a MEMS technique, by a drop coating technique employing an air-pulse fluid dispenser with a syringe of suitable size. Then, the microsensor chips were fired at 500 °C for 3 h in air. The thickness of the oxide films was controlled to approximately 30 μm. Hereafter, the sensor will be referred to, depending on the type of sensing material (namely, WO_3, mNiO/WO_3, or nN/mNiO/WO_3).

The gas responses of these sensors were measured with 20 ppm acetone and 20 ppm H_2 balanced with air under dry and wet [relative humidity (RH): 50% at 30 °C] atmospheres at a flow rate of 100 cm^3min^{-1}. These sensors were mainly operated in dynamic temperature modulation mode. The operating temperature was dynamically controlled by the sinusoidal modulation of heater voltage (V_h) with the amplitude of 0–$V_{h,max}$ V [$V_{h,max}$: maximum of V_h, 0.6 V (for 150 °C)–1.6 V (for 400 °C)] and a period of 6 s, and the maximum temperature achieving $V_{h,max}$ in one period was denoted as T_{max}. Dynamic sensor response [$R_{D(TG)}$, target gas (TG): acetone (Ac) or H_2] was defined as the ratio of sensor resistance in 20 ppm acetone or 20 ppm H_2 balanced with air to that in air at each T_{max}. Dynamic acetone selectivity against H_2 (S_D) was defined as a ratio of $R_{D(Ac)}$ to $R_{D(H_2)}$. The sensors were operated during 10 cycles in the sinusoidal modulation mode, and the $R_{D(TG)}$ and S_D were calculated at the last cycle. The static sensing properties of some sensors to 20 ppm acetone

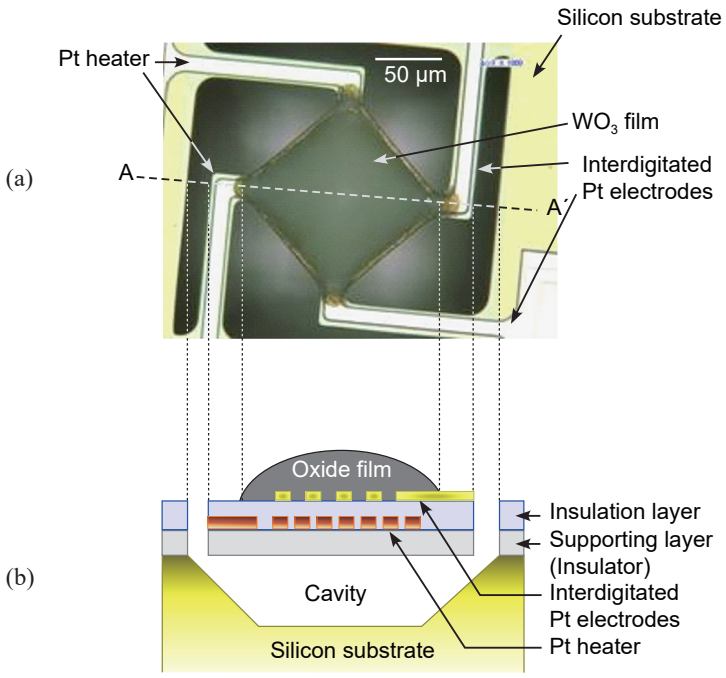

Fig. 1. (Color online) (a) Top view of typical micro gas sensor (gas-sensing material: WO_3) and (b) cross-sectional schematic drawing of region between A and A′ of micro gas sensors fabricated in this study.

and H_2 were also measured at constant temperatures (150–400 °C). Static sensor response ($R_{S(TG)}$) was defined as the ratio of sensor resistance in 20 ppm acetone or H_2 balanced with air to that in air at each constant operating temperature, and static acetone selectivity against H_2 (S_S) was defined as the ratio of $R_{S(Ac)}$ to $R_{S(H_2)}$.

3. Results and Discussion

Figure 2 shows the typical dynamic sensor-signal profiles of representative (WO_3 and 0.5Pt/WO_3) sensors in dry air and in 20 ppm acetone balanced with dry air, together with modulated heater voltage (V_h, 0–0.8 V) and operating temperature (T, RT–200 °C). The resistances of these sensors decreased with increasing V_h (namely, with a rise in T), and the resistances became the smallest at $V_{h,max}$ (0.8 V, T_{max}: 200 °C). The resistance of the WO_3 sensor in 20 ppm acetone balanced with dry air was smaller than that in air over the entire range of V_h (T), but the difference between the resistance in dry air and that in 20 ppm acetone balanced with dry air was much smaller than we had expected. The loading of Pt onto the WO_3 increased the sensor resistance in dry air and markedly decreased the sensor resistance in 20 ppm acetone balanced with dry air, especially in the temperature range of ca. 100–200 °C. This indicates that the dynamic sensor response to acetone ($R_{D(Ac)}$) of the 0.5Pt/WO_3 sensor was much larger than that of the WO_3 sensor in dry air. However, the resistance of the 0.5Pt/WO_3 sensor in 20 ppm acetone balanced with dry air was comparable to that in dry air in the low temperature range (near RT), because the sensor resistance was in such a very high range that we could not exactly measure the difference in sensor resistances between in air, and in 20 ppm acetone balanced with dry air.

Figure 3 shows the T_{max} dependences of responses to 20 ppm acetone and 20 ppm H_2 ($R_{D(Ac)}$ and $R_{D(H_2)}$, respectively) of WO_3 and 0.5*N*/WO_3 sensors in dry and wet air under dynamic temperature operation. The WO_3 sensor had little response to acetone and H_2 over the entire T_{max} range, regardless of whether moisture was added to the gaseous atmosphere. The Au loading onto the

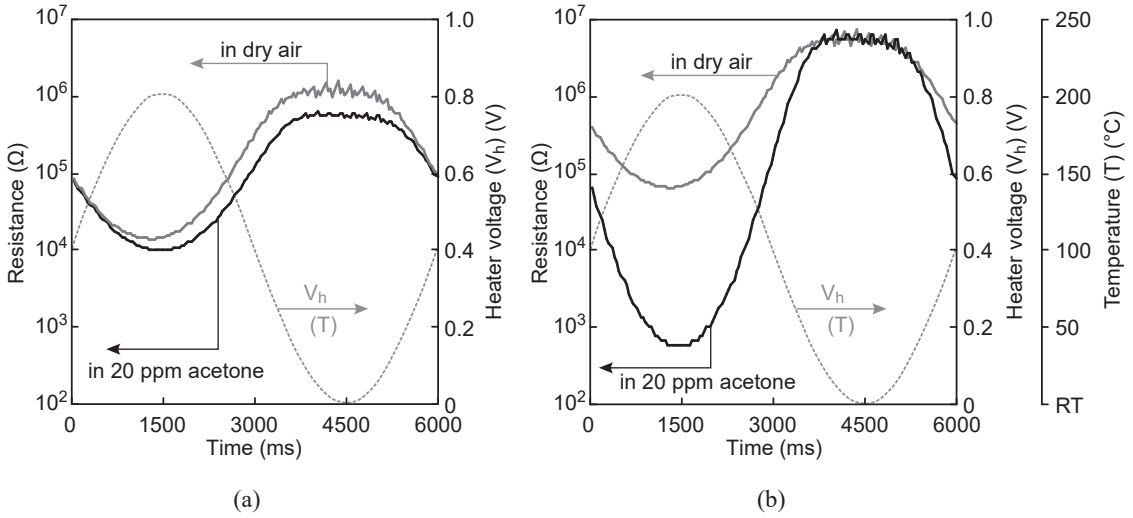

Fig. 2. Typical dynamic sensor-signal profiles of representative sensors in dry air and in 20 ppm acetone balanced with dry air, together with V_h and T. (a) WO_3 sensor. (b) 0.5Pt/WO_3 sensor.

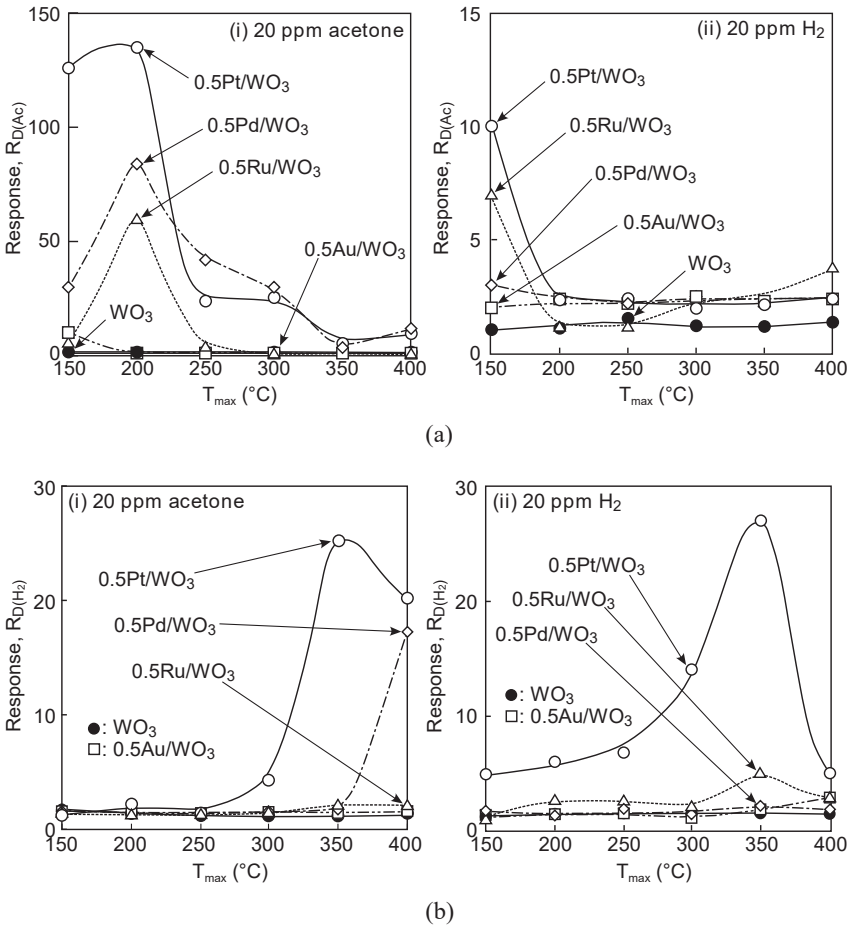

Fig. 3. Variations in responses of WO_3 and 0.5*M*/WO_3 sensors to 20 ppm acetone and 20 ppm H_2 in dry and wet air, with maximum temperature (T_{max}) under dynamic temperature operation. (a) In dry air. (b) In wet air.

WO_3 hardly improved $R_{D(Ac)}$ and $R_{D(H_2)}$ of the WO_3 sensor, but the loading of Pd, Pt, or Ru onto the WO_3 was effective in enhancing both responses. The 0.5*N*/WO_3 sensors (*N*: Pd, Pt, and Ru) showed relatively large acetone responses at low temperatures (especially at 200 °C) in dry air, but the addition of moisture into the gaseous atmosphere markedly reduced their $R_{D(Ac)}$ at low temperatures and enhanced their $R_{D(Ac)}$ in the temperature range of ca. 350–400 °C. On the other hand, the loading of Pd, Pt, or Ru onto WO_3 also tended to increase the $R_{D(H_2)}$ of these sensors in dry air at the lowest T_{max} (150 °C), while the addition of moisture into the gaseous atmosphere decreased the $R_{D(H_2)}$ at 150 °C and increased the $R_{D(H_2)}$ at 350 °C. The shift in T_{max} of the largest $R_{D(Ac)}$ and $R_{D(H_2)}$ from low temperature (200 °C) to high temperature (350–400 °C) by the addition of moisture into the gaseous atmosphere probably originates from the reduction in the catalytic combustion activities of acetone and H_2 over the gas-sensing materials (0.5*M*/WO_3, *N*: Pd, Pt, and Ru) by the adsorption of water molecules on the oxide surface. Among all the 0.5*M*/WO_3 sensors, the 0.5Pt/WO_3 sensor showed the largest $R_{D(Ac)}$ and $R_{D(H_2)}$, which were quite dependent on humidity in the gaseous atmosphere. Therefore, the excellent acetone selectivity of the 0.5Pt/WO_3 sensor against H_2 (S_D) at 200 °C in dry air (ca. 58) dropped to ca. 0.38 with the addition of moisture into the gaseous atmosphere, since

$R_{D(Ac)}$ (ca. 2.3) was smaller than $R_{D(H_2)}$ (ca. 6.0) at 200 °C in wet air. In addition, the relatively large $R_{D(Ac)}$ and $R_{D(H_2)}$ of the 0.5Pt/WO_3 sensor at 350 °C in wet air were not helpful in improving the S_D.

As mentioned above, the loading of the noble metal enhanced the magnitude of the acetone response of the WO_3 sensor, but it was not effective in reducing the effect of humidity on the acetone selectivity against H_2. Kim *et al.* have demonstrated that the humidity dependence of CO-sensing properties of SnO_2-based sensors is reduced to a negligible level by NiO loading onto the SnO_2 surface.[41] Therefore, NiO was dispersively loaded onto the WO_3 powder by impregnation employing $Ni(NO_3)_2$ to improve the acetone-sensing properties of the WO_3-based sensor in wet air. Figure 4 shows the T_{max} dependences of $R_{D(Ac)}$ and $R_{D(H_2)}$ of *m*NiO/WO_3 sensors (*m* = 1.0, 5.0, and 10) in dry and wet air, under dynamic temperature operation, together with those of the WO_3 sensor. The $R_{D(Ac)}$ in dry air gradually increased with an increase in the amount of NiO loading, especially at 300 and 400 °C, and the $R_{D(Ac)}$ of all *m*NiO/WO_3 sensors was apparently larger than $R_{D(H_2)}$ only at 400 °C in dry air. On the other hand, the loading of 1.0 wt% NiO onto WO_3 was quite effective in improving the $R_{D(Ac)}$ of the WO_3 sensor in wet air, but the further increase in the amount of NiO loading reduced the positive impact of the NiO loading on the $R_{D(Ac)}$ in wet air. As the $R_{D(H_2)}$ of all *m*NiO/WO_3 sensors in wet air was comparable to that of the WO_3 sensor, the 1.0NiO/WO_3

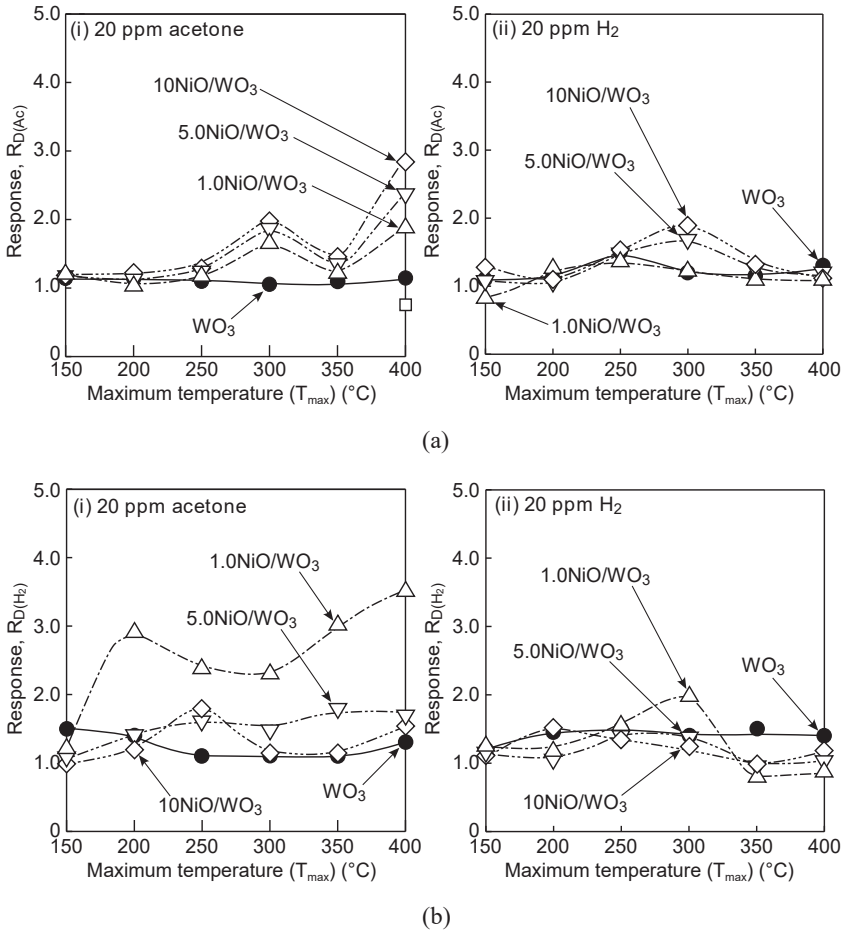

Fig. 4. Variations in response of WO_3 and *m*NiO/WO_3 sensors to 20 ppm acetone and 20 ppm H_2 in dry and wet air, with maximum temperature (T_{max}) under dynamic temperature operation. (a) In dry air. (b) In wet air.

sensor showed a relatively large S_D in the temperature range between 200 and 400 °C, among all the mNiO/WO_3 sensors.

We attempted to improve the acetone-sensing properties of the 1.0NiO/WO_3 sensor, which showed the largest $R_{D(Ac)}$ and S_D in wet air among all the mNiO/WO_3 sensors, by the loading of Pt onto the 1.0NiO/WO_3. Figure 5 shows the T_{max} dependences of $R_{D(Ac)}$ and $R_{D(H_2)}$ of nPt/1.0NiO/WO_3 sensors (n = 0.1, 0.5, and 1.0) in dry and wet air under dynamic temperature operation. The $R_{D(Ac)}$ of the nPt/1.0NiO/WO_3 sensors both in dry and wet air tended to be smaller than that of the 0.5Pt/WO_3 sensor (see Fig. 3), but the loading of Pt apparently enhanced both $R_{D(Ac)}$ and $R_{D(H_2)}$ of the 1.0NiO/WO_3 sensor (see Fig. 4). The 0.5Pt/1.0NiO/WO_3 sensor showed the largest $R_{D(Ac)}$ both in dry and wet air among all nPt/1.0NiO/WO_3 sensors, probably because the larger amount of Pt loading (*e.g.*, 1 wt%) onto WO_3 excessively enhanced the catalytic combustion properties of acetone over nPt/1.0NiO/WO_3 and thus the concentration of acetone at the bottom of 1.0Pt/1.0NiO/WO_3 films near interdigitated Pt electrodes of the sensor was lower than that of the 0.5Pt/1.0NiO/WO_3 film. On the other hand, the loading of Pt also enhanced the $R_{D(H_2)}$ of the 1.0NiO/WO_3 sensor (see Fig. 4), and the $R_{D(H_2)}$ of the nPt/1.0NiO/WO_3 sensors both in dry and wet air increased with increasing the amount of Pt loading, probably because the amount of H_2 oxidized on the surface of nPt/1.0NiO/

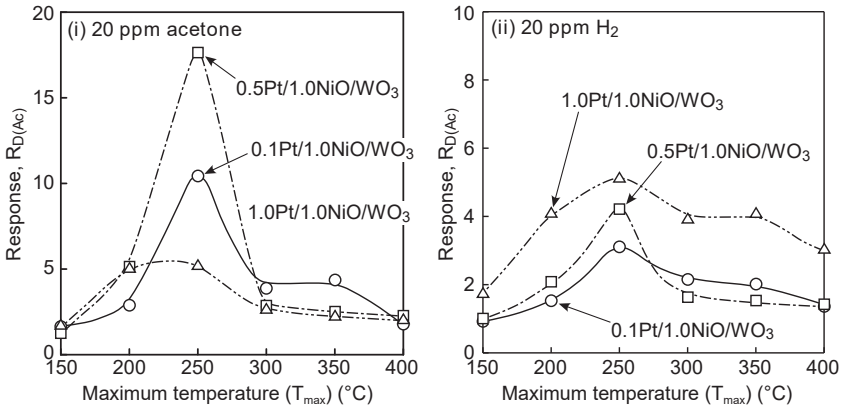

(a)

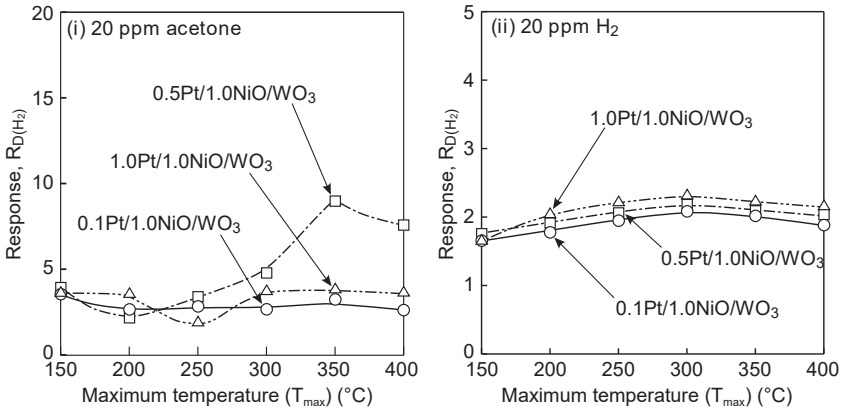

(b)

Fig. 5. Variations in response of nPt/1.0NiO/WO_3 sensors to 20 ppm acetone and 20 ppm H_2 in dry and wet air, with maximum temperature (T_{max}) under dynamic temperature operation. (a) In dry air. (b) In wet air.

WO_3 films was much smaller than that of acetone and thus the amount of H_2 that reacted with oxygen adsorbates on the *n*Pt/1.0NiO/WO_3 surface at the bottom side of the films was dependent on the amount of Pt loading. In addition, all the *n*Pt/1.0NiO/WO_3 sensors showed the largest $R_{D(Ac)}$ and $R_{D(H_2)}$ at lower T_{max} (250 °C) in dry air, but the addition of moisture into the gaseous atmosphere shifted T_{max} of the largest $R_{D(Ac)}$ and $R_{D(H_2)}$ from low temperature (200 °C) to high temperature (350–400 °C), as is the case with the 0.5Pt/WO_3 sensor. In addition, the 0.5Pt/1.0NiO/WO_3 sensor showed the most excellent S_D (*e.g.*, ca. 4.1 at 250 °C in dry air and ca. 5.2 at 350 °C in wet air) among all the mNiO/WO_3 sensors.

Representative (WO_3, 0.5Pt/WO_3, and 0.5Pt/1.0NiO/WO_3) sensors were statically operated at constant temperatures, and the static responses of these sensors to 20 ppm acetone and 20 ppm H_2 in dry and wet air were investigated, in comparison with the dynamic responses of these sensors operated in dynamic temperature modulation mode. Figure 6 shows the operating temperature dependence of static responses to 20 ppm acetone ($R_{S(Ac)}$) and 20 ppm H_2 ($R_{S(H_2)}$) of these sensors in dry and wet air. The WO_3 sensor had little $R_{S(Ac)}$ and $R_{S(H_2)}$ at all operating temperatures both in dry and wet air. The loading of 0.5 wt% Pt apparently enhanced the $R_{S(Ac)}$ in dry air, in comparison with the $R_{S(H_2)}$, but the effect of the Pt loading on the $R_{S(Ac)}$ in dry air was much smaller than that of the

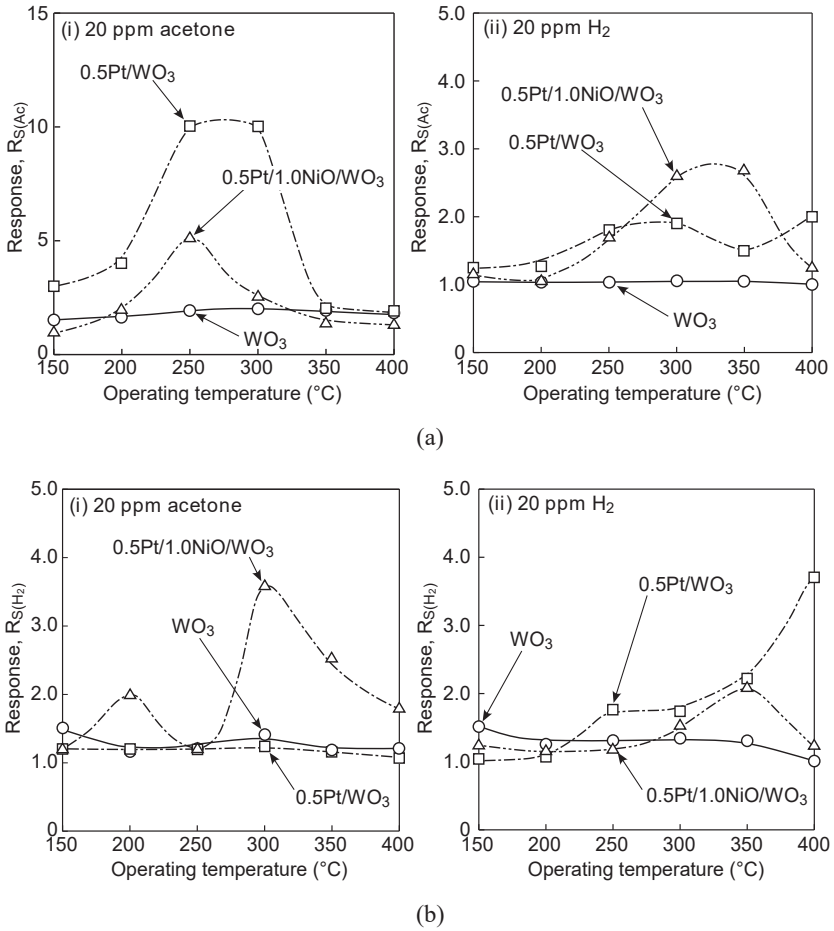

Fig. 6. Variations in response of WO_3, 0.5Pt/WO_3, and 0.5Pt/1.0NiO/WO_3 sensors to 20 ppm acetone and 20 ppm H_2 in dry and wet air, with operating temperature under static temperature operation. (a) In dry air. (b) In wet air.

dynamic response ($R_{D(Ac)}$) in dry air [see Fig. 3(a-i)]. In addition, the addition of moisture into the gaseous atmosphere markedly decreased the $R_{S(Ac)}$, as is the case with the $R_{D(Ac)}$. The $R_{S(H_2)}$ of the 0.5Pt/WO_3 sensor is also smaller than the $R_{D(H_2)}$, but the effect of humidity on the $R_{S(H_2)}$ seems to be limited in comparison with that on the $R_{D(H_2)}$. On the other hand, the $R_{S(Ac)}$ of the 0.5Pt/1.0NiO/WO_3 sensor was smaller than that of the 0.5Pt/WO_3 sensor and the $R_{D(Ac)}$ of the 0.5Pt/1.0NiO/WO_3 sensor in dry air [see Fig. 5(a-i)], while the effect of humidity on the $R_{S(Ac)}$ of the 0.5Pt/1.0NiO/WO_3 sensor (largest $R_{S(Ac)}$: ca. 5.1 at 250 °C in dry air, ca. 3.6 at 300 °C in wet air) was much smaller than that on the $R_{S(Ac)}$ of the 0.5Pt/WO_3 sensor. The $R_{S(H_2)}$ of the 0.5Pt/1.0NiO/WO_3 sensor was apparently larger than that of the 0.5Pt/WO_3 sensor only at 300 and 350 °C in dry air, but the addition of moisture into the gaseous atmosphere reduced the $R_{S(H_2)}$ at all the operating temperatures.

The temperature dependences of S_D and S_S of the WO_3, 0.5Pt/WO_3, and 0.5Pt/1.0NiO/WO_3 sensors under dynamic and static temperature operations, respectively, are summarized in Fig. 7. The 0.5Pt/WO_3 sensor showed the largest S_S under static temperature operation in dry air, but the S_S largely decreased with the addition of moisture into the gaseous atmosphere. The loading of NiO with Pt onto WO_3 decreased the S_S of the 0.5Pt/WO_3 sensor in dry air, but the S_S of the 0.5Pt/1.0NiO/WO_3 sensor was relatively larger than those of the WO_3 and 0.5Pt/WO_3 sensors

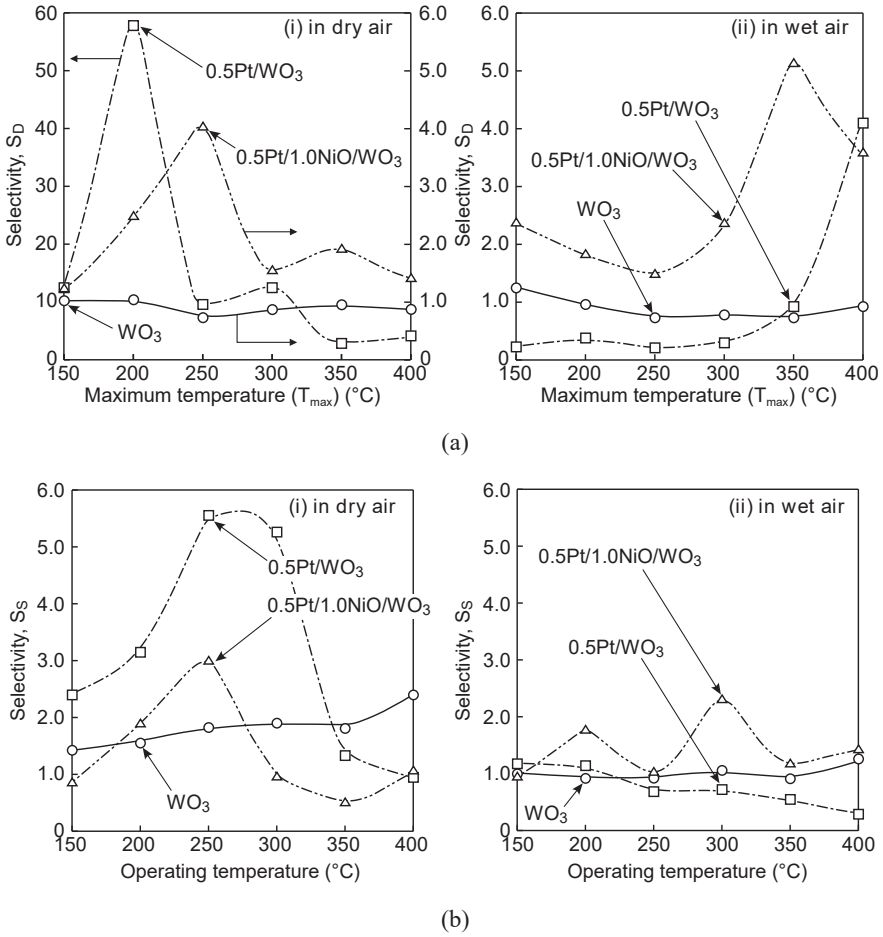

Fig. 7. Variations in acetone selectivity of WO_3, 0.5Pt/WO_3, and 0.5Pt/1.0NiO/WO_3 sensors against H_2 in dry and wet air, with T_{max} and operating temperature under dynamic and static temperature operations, respectively. (a) Dynamic operation (temperature modulation). (b) Static operation (constant temperature).

in wet air. This result indicates that the loading of NiO reduced the negative effect of moisture on the acetone selectivity against H_2 under static temperature operation. On the other hand, the S_D of the WO_3 sensor under dynamic temperature operation was smaller than its S_S under static temperature operation both in dry and wet air, while the S_D of the 0.5Pt/WO_3 sensor in dry air was largely improved by the dynamic temperature modulation. However, the S_D of the 0.5Pt/WO_3 sensor markedly decreased with the addition of moisture into the gaseous atmosphere. The S_D of the 0.5Pt/1.0NiO/WO_3 sensor, which was much smaller than that of the 0.5Pt/WO_3 sensor in dry air, increased at higher temperatures by the addition of moisture, and the 0.5Pt/1.0NiO/WO_3 sensor showed the largest acetone selectivity against H_2 with a relatively large acetone response [see Fig. 5(b-i)] when it was operated in dynamic temperature-modulation mode with T_{max} of 350 °C. The large acetone selectivity against H_2 (S_D) and the large acetone response ($R_{D(Ac)}$) of the 0.5Pt/WO_3 and 0.5Pt/1.0NiO/WO_3 sensors in dynamic temperature-modulation mode in dry air probably result from the effective adsorption of a large amount of acetone and/or the partial oxidation products on the Pt-loaded WO_3 surface in the temperature range between RT and the medium temperature (*e.g.*, one hundred and several tens of degrees Celsius) and subsequent abrupt catalytic combustion of these absorbates in the temperature range between medium temperature and T_{max}. In addition, the loading of NiO on the WO_3 improved the S_D and $R_{D(Ac)}$ of the WO_3 and 0.5Pt/WO_3 sensors in wet air. Kim *et al.* suggested that NiO-loaded SnO_2 sensors exhibit an excellent CO response that is independent of humidity (ca. 25%RH), because NiO loaded on the SnO_2 surface served as a strong humidity absorber and it protected the SnO_2 from being affected by water-derived species.[41] According to the discussion, the relatively large S_D and $R_{D(Ac)}$ of the 0.5Pt/1.0NiO/WO_3 sensor operated in dynamic temperature-modulation mode even in wet air may be associated with the selective adsorption of water molecules onto the NiO, which assisted the adsorption and subsequent catalytic combustion of acetone and/or its partial oxidation products onto active Pt/WO_3 regions on the 0.5Pt/1.0NiO/WO_3 sensor.

4. Conclusions

The acetone-sensing properties of WO_3, *m*NiO/WO_3, and *nN*/*m*NiO/WO_3 sensors operated in dynamic temperature mode with sinusoidal modulation of V_h {amplitude: 0–$V_{h,max}$ V [$V_{h,max}$: 0.6 V (for 150 °C)–1.6 V (for 400 °C)] and a period of 6 s} in dry and wet air have been investigated and the effects of the dynamic temperature operation and the coloading of Pt and NiO onto WO_3 on acetone response and acetone selectivity against H_2 have been clarified in this study. The $R_{D(Ac)}$ and $R_{D(H_2)}$ of the WO_3 sensor was negligible, but the loading of a noble metal onto the WO_3 was effective in improving the $R_{D(Ac)}$ and $R_{D(H_2)}$. The 0.5Pt/WO_3 sensor showed the largest $R_{D(Ac)}$ among all the 0.5*N*/WO_3 sensors tested in dry air, but the addition of moisture into the gaseous atmosphere markedly reduced the $R_{D(Ac)}$ of the 0.5Pt/WO_3 sensor. The loading of NiO improved the negative effect of moisture on the S_D as well as $R_{D(Ac)}$ of the WO_3 and 0.5Pt/WO_3 sensors, and the 0.5Pt/1.0NiO/WO_3 sensor showed the most excellent acetone-sensing properties in wet air. In addition, the operation of the sensors in dynamic temperature modulation mode effectively enhanced the acetone response and the acetone selectivity against H_2 in comparison with the operation in static constant temperature mode, probably because a large amount of acetone and/or the partial oxidation products adsorbed on the oxide surface at low temperatures and, subsequently, they reacted with oxygen adsorbates at high temperatures to decrease the resistance of the sensors.

References

1 L. F. McKay, W. P. Holbrook, and M. A. Eastwood: Acta Path. Microbiol. Immunol. Scand. Sect., B **90** (1982) 257.
2 M. Nishibori, W. Shin, N. Izu, T. Itoh, and I. Matsubara: Sens. Actuators, B **137** (2009) 524.
3 B. P. J. de Lacy Costello, M. Ledochowski, and N. M. Ratcliffe: J. Breath Res. **7** (2013) No. 024001.
4 W. Nq and J. Tonzetich: J. Dent. Res. **63** (1984) 994.
5 S. Persson, M.-B. Edlund, R. Claesson, and J. Carlsson: Oral Microbiol. Immunol. **5** (1990) 195.
6 L. R. Narasimhan, W. Goodman, and C. K. N. Patel: Proc. Nat'l Acad. Sci. U.S.A. **98** (2001) 4617.
7 K. Alving, E. Weitzberg, and J. M. Lundberg: Eur. Respir. J. **6** (1993) 1368.
8 Z. W. Weitz, A. J. Birnbaum, J. L. Skosey, P. A. Sobotka, and E. J. Zarling: The Lancet **337** (1991) 933.
9 N.-H. Kim, S.-J. Choi, D.-J. Yang, J. Bae, J. Park, and I.-D. Kim: Sens. Actuators, B **193** (2014) 574.
10 I.-D. Kim, S.-J. Choi, S.-J. Kim, and J.-S. Jang: Exhaled breath sensors in "Smart sensors for health and environmental monitoring (ed. by C.-M. Kyung)" (Springer, Heidelberg, 2015) pp. 19–49.
11 Y. Masuda, T. Itoh, W. Shin, and K. Kato: Sci. Rep. **5** (2015) No. 10122. doi: 10.1038/srep10122
12 S. K. Kundu, J. A. Bruzek, R. Nair, and A. M. Judilla: Clin. Chem. **3** (1993) 87.
13 C. Turner, C. Walton, S. Hoashi, and M. Evans: J. Breath Res. **3** (2009) No. 046004. doi: 10.1088/1752-7155/3/4/046004
14 Q. Qi, T. Zhang, L. Liu, X. Zheng, Q. Yu, and H. Yang: Sens. Actuators, B **134** (2008) 166.
15 M. Righettoni, A. Tricoli, and S. E. Pratsinis: Chem. Mater. **22** (2010) 3152.
16 M. Righettoni, A. Tricoli, and S. E. Pratsinis: Anal. Chem. **82** (2010) 3581.
17 L. Wang, K. Kalyanasundaram, M. Stanacevic, and P. Gouma: Sens. Lett. **8** (2010) 1.
18 D. Chen, X. Hou, T. Li, L. Yin, B. Fan, H. Wang, X. Li, H. Xu, H. Lu, R. Zhang, and J. Sun: Sens. Actuators, B **153** (2011) 373.
19 P. Gao, H. Ji, and X. Li: Thin Solid Films **520** (2012) 310.
20 I. Lee, S.-J. Choi, K.-M. Park, S. S. Lee, S. Choi, and I.-D. Kim: Sens. Actuators, B **197** (2014) 300.
21 W. Tang, J. Wang, Q. Qiao, Z. Liu, and X. Li: J. Mater. Sci. **50** (2015) 2605.
22 C. Wang, J. Liu, Q. Yang, P. Sun, Y. Gao, F. Liu, J. Zheng, and G. Lu: Sens. Actuators, B **220** (2015) 59.
23 Y. Xie, R. Xing, Q. Li, L. Xu, and H. Song: Sens. Actuators, B **211** (2015) 255.
24 A. Heilig, N. Bârsan, U. Weimar, M. Schweizer-Berberich, J. W. Gardner, and W. Göpel: Sens. Actuators, B **43** (1997) 45.
25 A. P. Lee and B. J. Reedy: Sens. Actuators, B **60** (1999) 35.
26 J. Lerchner D. Caspary, and G. Wolf: Sens. Actuators, B **70** (200) 57.
27 A. Ortega, S. Marco, A. Perera, T. Šundic, A. Pardo, and J. Samitier: Sens. Actuators, B **78** (2001) 32.
28 K. Yoshikawa: Chem. Sens. **18**(A) (2002) 25.
29 X. Huang, F. Meng, Z. Pi, W. Xu, and J. Liu: Sens. Actuators, B **99** (2004) 444.
30 S. Nakata, H. Okunishi, and Y. Nakashima: Sens. Actuators, B **119** (2006) 556.
31 K. An, Ngo, P. Lauque, and K. Aguir: Sens. Actuators, B **124** (2007) 209.
32 E. Martinelli, D. Polese, A. Catini, A. D'Amico, and C. Di Natale: Sens. Actuators, B **161** (2012) 534.
33 R. Gosangi and R. Gutierrez-Osuna: Sens. Actuators, B **185** (2013) 201.
34 F. Herrero-Carrón, D. J. Yáñez, and F. de Borja Rodríguesz: Sens. Actuators, B **206** (2015) 555.
35 T. Sasahara, M. Nishimura, H. Ishihara, K. Toyoda, T. Sunayama, S. Uematsu, T. Ozawa, K. Ogino, and M. Egashira: Electrochemistry **71** (2003) 457.
36 T. Sasahara, A. Kido, T. Sunayama, S. Uematsu, and M. Egashira: Sens. Actuators, B **99** (2004) 532.
37 T. Sasahara, H. Kato, A. Saito, M. Nishimura, and M. Egashira: Sens. Actuators, B **126** (2007) 536.
38 Y. Yuzuriha, T. Hyodo, T. Sasahara, Y. Shimizu, and M. Egashira: Sens. Lett. **9** (2011) 409.
39 T. Hyodo, Y. Yuzuriha, O. Nakagoe, T. Sasahara, S. Tanabe, and Y. Shimizu: Sens. Actuators, B **202** (2014) 748.
40 T. Hyodo, T. Hashimoto, T. Ueda, O. Nakagoe, K. Kamada, T. Sasahara, S. Tanabe, and Y. Shimizu: Sens. Actuators, B **202** (2014) 748.
41 H.-R. Kim, A. Haensch, I.-D. Kim, N. Barsan, U. Weimar, and J.-H. Lee: Adv. Funct. Mater. **21** (2011) 4456.